Experimental validation of an image-based dynamic pore-network model for spontaneous imbibition in sandstones

Hardener-Dependent Properties of Twice Renewable Epoxy Resins Combining Tailored Lignin Fractions and Recycled BPA

Journal:	*ACS Sustainable Chemistry & Engineering*
Manuscript ID	sc-2024-02394r.R2
Manuscript Type:	Article
Date Submitted by the Author:	15-May-2024
Complete List of Authors:	Comí, Marc; Flemish Institute for Technological Research, Materials and Chemistry Unit Van Ballaer, Brent; Flemish Institute for Technological Research, Materials and Chemistry Unit Gracia Vitoria, Jaime; Flemish Institute for Technological Research, Materials and Chemistry Unit Parida, Dambarudhar; Flemish Institute for Technological Research, Materials and Chemistry Unit Aerts, Annelore; Flemish Institute for Technological Research, Materials and Chemistry Unit Vanbroekhoven, Karolien; Flemish Institute for Technological Research, Materials and Chemistry Unit Vendamme, Richard; Flemish Institute for Technological Research, Materials and Chemistry Unit

Hardener-dependent properties of twice renewable epoxy resins combining tailored lignin fractions and recycled BPA

Marc Comí,[a*] Brent van Ballaer,[a] Jaime Gracia-Vitoria,[a] Dambarudhar Parida,[a] Annelore Aerts,[a] Karolien Vanbroekhoven[a] and Richard Vendamme.[a*]

[a] Flemish Institute for Technological Research (VITO N.V.), Boeretang 200, Mol 2400, Belgium.

*Corresponding author. Tel: +32 14 33 69 72; email address: marc.comibonachi@vito.be and richard.vendamme@vito.be

Keywords: Kraft Lignin, Recycling, Coatings, Crosslink Density, Epoxy Resins, Hardener.

Keywords: biobased, sustainable, epoxide, coatings, crosslink density, curing, adhesion

ABSTRACT: The use of bio-sourced and/or recycled raw materials represents a promising strategy for making the polymer industry more renewable. In this context, both biobased lignin fractions and chemically recycled Bisphenol A (r-BPA) have been independently considered as promising renewable alternatives to aromatic fossil monomers. Here, renewable thermosetting epoxies were designed by combining tailored lignin fractions and rBPA, while the influence of several hardeners on the physical structure and properties of the obtained resins was systematically investigated. To do so, the phenolic groups of r-BPA derived from polycarbonate waste and of solvent-extracted Kraft lignin (EKL) were both glycidylated with epichlorohydrin (ECH). This lead to the renewable epoxy precursors r-BPA diglycidyl ether (r-DGEBA) and glycidylated extracted Kraft lignin (GEKL), respectively. Twenty different formulations were then designed by tailoring the structural parameters of the resins, such as the hardener length and functionality, the epoxide:hardener (E:H) ratio and the lignin content. The thermomechanical properties were investigated, and the structure-property relationships established, highlighting the excellent and tunable performance of these renewable epoxies. Finally, flexible coatings were produced with lower crosslink density formulations that demonstrated excellent performance, even with 30% of lignin content. Overall, our results show how biobased and recycled aromatic building blocks could be combined for the design of epoxy resins with superior properties, both in sustainable and technical terms.

Introduction

Almost a century after their invention, epoxy resin thermosets still represent a prominent family of versatile and durable synthetic polymers that have found widespread applications in various industries, thanks to their remarkable adhesive properties, excellent electrical insulation, and superior resistance to heat and chemicals. Their ability to form strong, durable bonds with different substrates makes them ideal for applications as diverse as art, automotive, construction, electronics, and aerospace. Their popularity is also based on their ease of molding, low shrinkage during curing, and ability to create a protective barrier against environmental factors, satisfying the advanced specifications expected in adhesives, coatings, and material encapsulation.[1] Despite their advantageous properties, traditional epoxy resins are still derived from glycidylated bisphenol A (BPA), which raises certain issues. At first, BPA is still entirely derived from petroleum feedstocks that are being depleted. Then, BPA is also raising environmental and health concerns for being an endocrine disruptor. These concerns are pushing both academia and industry to develop strategies for enhancing the sustainability of BPA-based epoxy resins, such as i) finding biobased alternative building blocks to (partially) replace BPA in epoxy resin formulations, ii) preventing BPA from ending up in landfill and leaching into the environment, and iii) chemically recycling BPA-based polymers and up-cycling the obtained recycled BPA (r-BPA) toward new high-value applications (e.g., such as coatings).[2, 3]

Plastic chemical depolymerization allows the end-of-life material to be fragmented chemically, efficiently producing the original monomers, which can be purified and used for new applications.[4] The principal limitations involve the purity of the waste material, solubility, accessibility to the internal structure and capability to break the targeted bonds.[5, 6] Polycarbonates from transparent screens and plates produced globally in large scale, especially during the COVID restrictions period, represented the perfect material candidates to attempt this chemical recycle methodology.[7] Thus, our group was motivated to efficiently produce high-quality recycled bisphenol A (r-BPA) from polycarbonate waste, considering previously reported methodologies.[8-10x] The obtention and repurpose of r-BPA could relax the utilization of fossil-based raw chemicals, promote the recyclability of similar plastics, and consequently, dramatically reduce the BPA environmental impact.[11]

A complementary strategy to prevent BPA-derived waste could involve using biobased alternatives to produce more sustainable epoxy resin, which is vital for a material industry in continuous expansion.[1] From the perspective of chemical structure similarity with BPA, biobased small molecules such as eugenol and vanillin have been proposed as suitable candidates,[12-15] but their high obtention price, availability and modification process limit the upscaling production.[16] In recent years, lignin biopolymer has attracted significant interest as a biobased candidate due to its three-dimensional structure rich in aromatics and active phenolic groups, which provides rigidity, strength, and reactive points.[17, 18] Additionally, lignin is the most abundant natural aromatic biopolymer and around 85 % of the total global production is originated as a byproduct from the Kraft pulp process for paper production.[19, 20] For the time being, the Kraft lignin is regarded as waste and incinerated to partially recuperate the operational energy from the pulp process, which makes the valorization of Kraft lignin into high-value products a suitable biobased alternative to BPA for the production of more sustainable epoxy resins.[21] To avoid processability issues and to achieve a major resemblance with the BPA molecule, Kraft lignin is generally fractionated to drastically reduce the molecular weight, improve the number of active functional groups, and enhance the solubility.[22] This process relies on the hydrolysis of internal ether bonds, such as β-O-4, to produce new aliphatic and phenolic alcohols. An increase of the lignin phenolic content has demonstrated to gratefully assist the epoxidation process, providing more reactivity to the resulting glycidylated biobased monomer.[23]

Despite the similarities with glycidylated bisphenol A (DGEBA), the utilization of glycidylated lignin (GL) in a resin epoxy formulation present several challenges that must be considered, such as process reproducibility, mixture uniformity, and crosslink contribution. The macromolecular statistical structure and polydispersity of Kraft lignin depends on a large number of parameters, such as the botanical origin (e.g., hardwood vs. softwood), biorefining process, operational batch, fractionation treatment, and functionalization methodology, among others. This affects the replicability of the epoxy resin fabrication, as has been widely reported.[24, 25] Moreover, in order to avoid phase separation and irregularities on the resulting biobased epoxy resins, the proper selection of formulation mixture is pivotal and presents few limitations commonly related with the dispersion of the GL. These are usually addressed by balancing the biobased content, and the

affinity between the epoxide (BPA, GL, other epoxide compounds) blend with the hardener, since drastic differences in structure (molecular weight, polarity, solubility) typically lead to heterogeneous crosslinks and alter the final properties.[26-28] The most impacting factor on the material properties is related to the lignin incorporation in a typical crosslink network (BPA:hardener) since the use of this biobased moiety as a partial replacement of BPA will modify the final material properties. The study of systematic alterations in the crosslink density of epoxy resins and understanding its correlation to thermal and mechanical performance is essential. It allows the selection of the best internal crosslink structure for a targeted application.

The transition to more sustainable epoxy resins with lower carbon footprints should be accompanied by an enhancement of the material's physical properties, understanding the structure-function relation based on the resin composition and benchmarking application tests. Among the numerous functions, lignin-based epoxy resins could provide excellent performances as coatings, where a low CO_2 footprint is crucial, the recyclability is not a primary target and this application is attracting significant attention.[29] The remaining phenol groups within lignin serve as effective scavengers of radicals, preventing oxidation reactions, and work as chromophores capable of absorbing UV light, promoting the protection barrier capabilities. While the aliphatic alcohols assist the material-substrate adhesion by forming H-bonds or strong polar attractions to oxide or hydroxyl surfaces.[30, 31]

Herein, we have designed and characterized a family of twenty renewable epoxy resins by systematically modulating the structural parameters of the formulations, such as the hardener chemical structures, the epoxide:hardener (E:H) ratios, and the content of extracted Kraft lignin (**EKL**) contents. In order to maximize the renewability of the epoxy resins, a recycled bisphenol A (r-BPA, obtained by solvolysis of PC) was combined with extracted Kraft lignin (EKL). The functionalization of both compounds using epichlorohydrin (ECH) yielded glycidylated kraft lignin (**GEKL**) and bisphenol A diglycidyl ether (**r-DGEBA**) that were combined with linear diamino-based hardeners to synthesize the series of epoxy resin material **Ref1-5** and **ER1-15**. Structural characterization using nuclear magnetic resonance (NMR), Fourier transform infrared (FT-IR), gel permeation chromatography (GPC) and complementary chemical analysis confirmed the quality and reproducibility of the process. The material curing conditions were established after the

evaluation of the formulation mixtures thermal behavior by DSC. Thermal and mechanical properties of the final epoxy resin series were investigated using DMA and tensile test analysis. Afterwards, the data extracted was compared to establish a close relationship with the material internal network structure. Finally, a metal coating was selected for application. The coating was prepared and the adhesion of the lignin-based epoxy resins to the substrate was tested. With this study, we have illustrated the combined use of recycled and biobased building blocks to deliver renewable materials with improved properties, anticipating applications in search for alternatives to fossil resources. Moreover, this work allows the prediction of the properties of lignin-based-epoxy resins by simply exchanging some parameters in the formulation that affect the crosslink density of the material which could alter the performance in a designated application.

Results and Discussion

Molecular Design, Synthesis and Characterization of Renewable Epoxy Precursors.

The steps followed in the preparation of the epoxide monomers are depicted in **Figure 1** and the complete methodology is described in *Supporting Information*, *Experimental Procedures* (**Table S1-2** and **Figure S1-3**). As previously reported, polycarbonate waste from transparent screens and panels was selected, washed, treated, and depolymerized.[9, 10] High purity r-BPA crystals were isolated after precipitation of the depolymerization mixture in toluene. The r-BPA was functionalized with ECH in basic conditions, obtaining r-DGEBA in good yields (> 90 %), as uncolored powder after column purification and dry under vacuum (**Figure 1a**).[32]

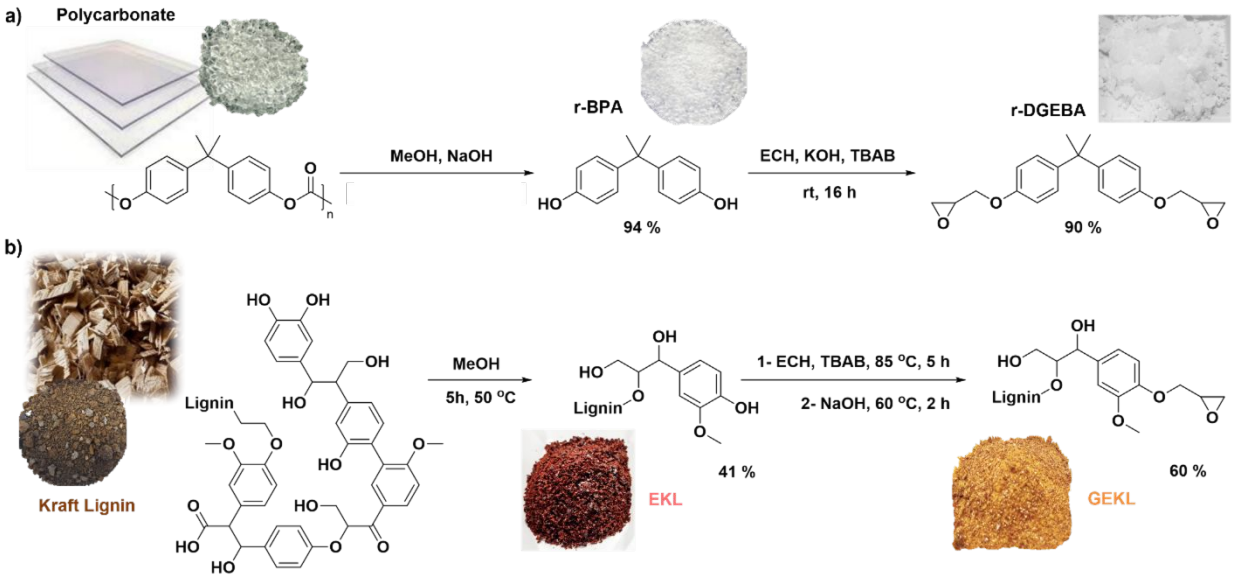

Figure 1. Scheme of the **r**outes used from waste source to epoxide monomers with photographs of the compounds: (**a**) PC, r-BPA and r-DGEBA, and (**b**) Kraft Lignin, **EKL** and **GEKL**.

As observed in the first part of **Figure 1b**, Kraft lignin was fractionated in methanol at 50 °C and after 5 h, the soluble part (up to 40 %) was isolated, dried, and characterized. This methodology was repeated three times and the extracted Kraft lignin (**EKL1-3**) samples exhibited suitable molar masses (M_n) ranging from 0.95 to 1.15 Kg/mol with values of polydispersity (Đ) in all cases close to 2, as summarized in **Table S1.** The hydroxyl content was calculated from the peak integration of the ^{31}P NMR spectra for **EKL1-3** samples, considering the diverse reactivity of each hydroxyl group to the phosphorylating agent.[33, 34] As shown in **Table S1**, similar results were obtained for the three methanol extraction attempts (**EKL1-3**), which confirms the reliability of the process. Noteworthy, in the **EKL1-3** samples, the phenolic groups were estimated to comprehend the majority of the hydroxyl groups (ranging 60-65 % from the total), benefiting a high further functionalization. For the second part of the process, **EKL1** powder was solubilized and reacted with ECH to produce glycidylated lignin dark syrup, following a similar two-step methodology previously reported.[28, 35] The dark syrup was precipitated in diethyl ether and dried under vacuum to obtain **GEKL1-3**, as a light brown solid powder (yield ranging 60-63 %). The **GEKL 1-3** structures were characterized by ^{31}P NMR and the absence of peaks in the phenolic and carboxylic acid region, between 134-145 ppm (**Figure S1**), confirmed the glycidylation of these functional groups.[25] Moreover, FT-IR examination of glycidylated lignin demonstrated a

noticeable reduction in the stretching vibrations of hydroxy groups at approximately 3400 cm^{-1} (as depicted in **Figure S2**), corroborating the phenolic and carboxylic acid modification. Furthermore, a new peak emerged at 905 cm^{-1}, a characteristic asymmetric stretching vibration associated with the C-O-C bonds in epoxide groups. In addition, several new peaks within the 1000 to 1250 cm^{-1} range appeared for **GEKL1**, these vibrations were associated with the newly created C-O-glycidyl bonds. The findings aligned with FT-IR spectra of glycidylated lignin compounds previously reported.[36, 37] Despite the slight increase in the molar mass of **GEKL1-3** after functionalization (≈0.5 kg/mol), the polydispersity remained uniform (as shown in **Figure S3**). The **GEKL1-3** samples displayed an EEW ranging from 331 to 341 g/eq,[28] with almost no ECH-derived impurities, as summarized in **Table S2**.

Design Rationale, Formulation, and Network Development of the Cured Epoxy Resins.

Three parameters were selected in order to systematically tune the macromolecular structure of the epoxy materials, as depicted in **Figure 2**: i) the amount of lignin in the formulation (which we further defined as the substitution ratio of r-BADGE by GL), ii) the structure of the hardener, and iii) the epoxy hardener (E:H) ratio.

i) The first parameter to be modified was the amount of lignin in the mixture, knowing that an excess of rigid and compact moieties of lignin in the formulation of the components could be highly detrimental to the mechanical properties of the epoxy resin. Furthermore, a physical limitation existed during the material preparation, where large amounts of lignin dramatically raised the viscosity of the monomer dispersion. That fact affected the uniformity in the material structure by presenting visible lignin agglomerations (**Image S1a**). Considering these observations, the lignin content in the epoxide monomer mixture was delimited to 0, 10, 20 and 30 % (**a**).

ii) The second parameter to be compared is the hardener structure, particularly the length of the flexible chain between the telechelic amine groups, which was expected to balance the introduction of lignin by conferring ductility to the material. The initial idea of the study was to systematically compare the Jeffammine (Jeff) series D230, D400, and D2000, which all display the same linear structure but with different lengths of flexible middle chains. However, dramatic

phase separation was observed for samples containing Jeff D2000. Despite several attempts to improve the mixture preparation, the uniformity of the obtained materials was poor, especially for specimens containing 20 and 30 % lignin, as shown in **Image S1b**. Therefore, the hardeners selected for the epoxy resin fabrication were 1,6-hexamethylenediamine (HDA), Jeff D230, and Jeff D400 (**b**).

iii) Finally, the E:H ratio was selected as the third design parameter. In an ideal scenario, when E:R ratio = 4:2, every single diamine will react with four epoxide groups, making the hardener fully act as a crosslinking agent of the polymeric system. In order to evaluate the crosslinking capability of the glycidylated lignin, higher amounts of hardener were added to the formulation. This way, it increased the probability of the amine groups reacting only with one epoxide group, allowing the lignin moiety to act partially as a crosslinker. Additionally, this modification enhanced the reaction mixture's fluidity and greatly facilitated the material preparation. The E:H ratios selected were 4:2, 3:2 and 2:2, where 4, 3 or 2 epoxide groups were expected to react for each equivalent of hardener (2 amine groups), respectively (**c**).

Overall, a collection of 20 epoxy bio-resins with differentiated structures were fabricated according to the previously mentioned design parameters: 5 specimens did not contain lignin and were named references (**Ref1-5**), while the 15 remaining samples contain 10-30 % of lignin and were called epoxy resin (**ER1-15**) samples, as represented on **Scheme 2**. The variations on hardener structure, E:H ratio and lignin content for each epoxy resin is summarized in **Table 1**.

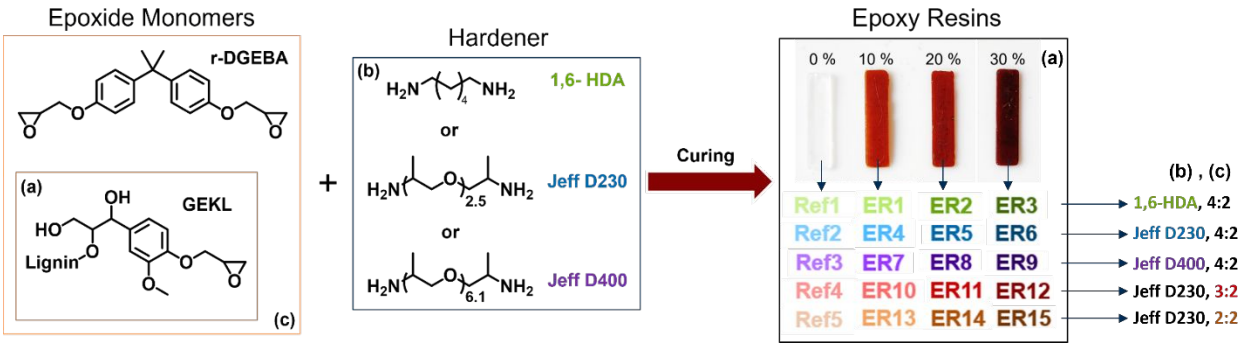

Figure 2. Schematic representation of the parameters altered in the formulation (a) lignin content (0, 10, 20, 30 %), (b) hardener type (1,6-HDA, Jeff D230, Jeff D400) and (c) E:H ratio (4:2, 3:2 and 2:2) leading to the 20 epoxy resins fabricated (**Ref1-5**, **ER1-15**). Photography of **Ref2**, **ER4**, **ER5** and **ER6** epoxy resin samples.

Table 1. Summary of composition, thermal and mechanical parameters from the synthesized epoxy resin specimens.

Epoxy resin	Formulation parameters			DSC	Dynamic Mechanical Analysis				Tensile test		
	GELK (%)	Hardener type	Epo/Hard ratio	T_g (°C)	E' at -25^{0}C (MPa)	E' at 150^{0}C (MPa)	T_g (^{0}C)	v_e (mmol/cm^3)	E_{young} (GPa)	σ_{UTS} (MPa)	ε_{break} (%)
Ref1	0	1,6-HDA	4\2	86	4583.57	54.61	122	5.17	2,2 ± 0,1	79 ± 3	4.6 ± 0,2
ER1	10	1,6-HDA	4\2	91	3437.72	24.01	103	2.27	1,9 ± 0,1	70 ± 3	5.1 ± 0,3
ER2	20	1,6-HDA	4\2	99	4104.29	28.96	108	2.74	2,3 ± 0,1	81 ± 5	4.4 ± 0,2
ER3	30	1,6-HDA	4\2	101	3917.81	25.67	108	2.43	2,4 ± 0,1	86 ± 4	4.2 ± 0,2
Ref2	0	Jeff D230	4\2	82	2961.67	15.26	82	1.45	1,9 ± 0,1	61 ± 2	10.2 ± 0,9
ER4	10	Jeff D230	4\2	83	3291.53	17.75	86	1.68	2,0 ± 0,1	66 ± 2	9.6 ± 0,6
ER5	20	Jeff D230	4\2	83	3766.11	16.45	90	1.56	2,3 ± 0,1	72 ± 3	8.5 ± 0,7
ER6	30	Jeff D230	4\2	80	3522.14	15.90	88	1.51	2,5 ± 0,1	81 ± 4	5.3 ± 0,2
Ref3	0	Jeff D400	4\2	48	3267.29	11.81	47	1.12	1,4 ± 0,1	50 ± 2	19.3 ± 2,0
ER7	10	Jeff D400	4\2	52	3260.82	15.00	50	1.42	1,8 ± 0,1	55 ± 2	15.9 ± 0,7
ER8	20	Jeff D400	4\2	58	3798.01	19.48	53	1.85	2,1 ± 0,1	60 ± 3	12.0 ± 0,9
ER9	30	Jeff D400	4\2	55	3934.80	22.86	54	2.17	2,2 ± 0,2	76 ± 3	10.2 ± 0,7
Ref4	0	Jeff D230	3\2	53	3661.35	10.33	60	0.98	1,8 ± 0,1	57 ± 2	15.4 ± 0,8
ER10	10	Jeff D230	3\2	56	4206.80	12.59	60	1.19	2,0 ± 0,1	61 ± 3	10.6 ± 0,8
ER11	20	Jeff D230	3\2	60	3702.08	13.98	63	1.32	2,2 ± 0,1	66 ± 3	7.7 ± 0,6
ER12	30	Jeff D230	3\2	63	3975.90	14.14	68	1.34	2,3 ± 0,1	76 ± 3	4.5 ± 0,1
Ref5	0	Jeff D230	2\2	34	3336.79	1.86	46	0.18	1,0 ± 0,1	28 ± 1	89.2 ± 5,0
ER13	10	Jeff D230	2\2	33	3555.24	2.87	50	0.27	1,3 ± 0,1	34 ± 1	26.9 ± 0,9
ER14	20	Jeff D230	2\2	34	3795.32	4.95	52	0.47	1,6 ± 0,1	48 ± 1	13.4 ± 0,9
ER15	30	Jeff D230	2\2	39	4341.30	7.65	54	0.72	2,0 ± 0,1	63 ± 2	6.6 ± 0,4

The curing conditions of the precursor mixtures were optimized to obtain fully reacted and homogeneous thermosetting materials. To do so, the curing exotherm of the epoxides-hardener mixtures was first screened by DSC to determine the maximum and the onset temperature of curing. **Figure S9** displays the DSC thermograms of the following systems: (**a**) different hardeners with r-DGEBA, (**b**) r-DGEBA: Jeff D230 system, different E:H ratio (top, dash line) and different lignin content (bottom, straight line). The structure of the hardener greatly influences the hardening temperature of the material. Notably, formulations comprising shorter linear hardeners react more quickly and at lower temperatures, which may be related to improved mobility in reactive formulations.

The formulations containing the short linear hardener 1,4-diaminobutane (DAB) consistently displayed somewhat similar thermogram curves, while the onset curing temperature for the Jeff D230 and D400 increased from 55 ^{o}C to 69 ^{o}C (ΔT=14°C) and 75 ^{o}C (ΔT=20°C), respectively. In addition, mixtures containing Jeff D230 and D400 as a hardener exhibited a broader exotherm curve than 1,6-HDA mixture, with maximums at 125 ^{o}C, 134 ^{o}C, and 100 ^{o}C respectively. Smaller difference presented the exotherm curves depicted in **Figure S9b**, by exchanging the E:H ratio and lignin content in the formulation seemed to have almost no effect in the onset curing temperatures and modest shift of the curing maximum. In light of the results, the curing conditions summarized in **Table S4** were applied to produce the epoxy resins, following the methodology described in the *Supporting Information*. The resulting samples showed no phase separation or visible defects, as shown in **Figure 2** for **Ref2**, **ER4**, **ER5** and **ER6** samples.

The samples were characterized by FT-IR and the spectra are included in *Supporting Information* **Figure S4-S8**. All the fabricated samples exhibited the common epoxy resin peaks.[38] Broad band above 3400 cm^{-1}, related largely to -OH stretching vibrations for all formulations, although materials **Ref4-5** and **ER10-15** including a major amount of hardener, this band can be overlayed with -NH stretching vibrations from amine groups unreacted. Three peaks assigned to symmetric and asymmetrical C–H stretching for methyl and methylene groups, respectively, appeared for all the samples in the range from 2920 to 2970 cm^{-1}. The region ranging 1600-1700 cm^{-1} and the two intense peaks around 1450 and 1510 cm^{-1} are typically associated with aromatic skeletal vibrations combined with C-H in-plane deformation.[39, 40] Between 1000-1400 cm$^{-1,}$ all the samples

exhibited a series of peaks related to C-C and C-H linkage vibration in aromatic moieties combined with C-O stretch for secondary alcohol, and including methoxy groups, in the cases of **ER1-15**, which incorporate lignin. The last peak around 830-840 cm^{-1} was assigned to aromatic C-H out-of-plane deformation.[41]

In addition, the thermal analysis by DSC confirmed the complete curing of all the epoxy resins since the thermograms, depicted in **Figure S10-S14**, showed total absence of curing exotherm while exhibiting a clear glass transition, with values of T_g summarized in **Table 1**. In general, results revealed lower T_g by increasing the hardener length for the different materials. This is related to the fact that longer chain moieties in the epoxy resin system provided more mobility at lower temperatures. A similar trend occurred with materials containing large amount of hardener, **Ref4-5** and **ER10-15**, the partial reactivity of the hardener amine groups provided less crosslink points and enhanced the mobility of the epoxy resin structure, decreasing the T_g around 30 and 50 ^oC, respectively, in comparison with **Ref2**, **ER4-6** samples. Otherwise, the increment of lignin in the formulation led to a slight increase in the T_g, mainly related with the reduction in chain mobility due to inclusion of the lignin rigid structure.

Epoxy Resins Thermo-Mechanical Profiles and Structure-Property Relationships.

The thermo-mechanical properties of the synthesized materials (**Ref1-5** and **ER1-15**, c.f. summary in **Table 1**) were then investigated by DMA in the temperature range (-50 ^oC to 200 ^oC) to elucidate their structure-property relationships. The thermal range of the analysis was selected to cover the glassy state, thermal transition, and rubbery region for all the samples. The DMA profiles of the epoxy resin illustrating the (**a**) storage modulus and (**b**) Tan δ/loss modulus are included in **Figure 3** and **Figure S15-S19** (*Supporting Information)*. All samples show the typical thermoset thermomechanical curve, where storage modulus (E') presented a glassy region at low temperatures, followed by a thermal transition, which ended in a rubbery plateau. Additionally, all the epoxy resins exhibit only one peak of Tan δ, that fact confirmed the high homogeneity of the crosslink (no phase separation) in the final material and corroborated the success during the component mixtures and curing methodology. Noteworthy, slightly broader profiles were

observed in the Tan δ curves due to the increment of the lignin content in the formulation from 0 to 30 % for all groups of epoxy resin fabricated. Besides, as the temperature increases, significant regions of the polymer exhibit cooperative movement, and the dissipated energy escalates, yet concurrently, the material as a whole becomes more susceptible to deformation, and the loss modulus (E'') reaches a peak in the order of 10^2 MPa for all the fabricated epoxy resins, as have been reported in previous studies.[25]

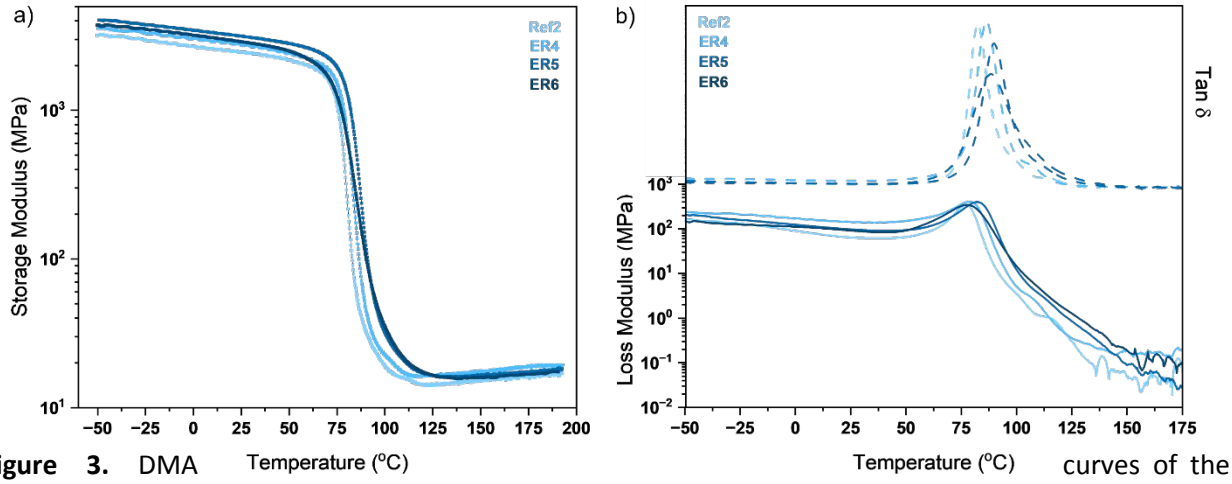

Figure 3. DMA curves of the heating ramp from -50 to 200 °C representing (a) storage modulus and (b) tan δ (dash line) and loss modulus (straight line) for **Ref2**, **ER4**, **ER5**, and **ER6**.

Relevant data such as T_g, E' at glassy stage, E' at rubbery stage, and crosslink density (v_e) were extracted from the DMA thermograms and summarized in **Table 1**. Given the clarity of the peak definition in all cases, the maximum point of the Tan δ curve was considered as the T_g. Coherent trends (in agreement with previously obtained DSC results) confirmed that hardener with increasing length (1,6-HDA > Jeff D230 > Jeff D400) dramatically influenced the chains mobility and led to lower T_g values. Similarly, by decreasing the E:H ratio from 4:2 to 2:2, it is promoted a partial reactivity of the hardener amine groups, providing the polymer network with a smaller number of crosslink points and including a major quantity of long alkyl chains that enhance the polymer mobility.

Interestingly, the increment of lignin amount (0 to 30%) for the different polymer networks only appeared to alter drastically for the r-DGEBA/1,6-HDA system (**Ref1**, **ER1-3**), where the T_g

dropped 20 ^{o}C after incorporating to the material 10 % of lignin (from Ref1 T_g = 122 ^{o}C to ER1 T_g = 103 ^{o}C), which can be explained by the dense crosslink density of **Ref1** being disrupted with the incursion of lignin moieties for **ER1-3**. Despite the previous case, mild fluctuations (0 - 9 ^{o}C) of the T_g were observed for the accumulation of lignin (0 – 30 %) in the other epoxy resin groups (**Ref2-5**, **ER4-15**).

In order to compare the effect in the epoxy resin crosslink structure, the parameters E' at -25 ^{o}C (glassy state for all samples), E' at 150 ^{o}C (rubbery state for all samples) and v_e at 150 ^{o}C were represented in **Figure 4** in two bar graphs, comparing the hardener length **(a)** and the E:H ratio **(b)**, as well as the lignin content in the formulation mixtures. Only slight differences were observed in the glassy state, and all the samples kept a high stiffness expected for glassy thermosetting polymers with values of E' above 3 x 10^3 MPa.[28] On the contrary, in the rubbery state (defined here at 150 ^{o}C to facilitate the comparison), epoxy resin containing 1,6-HDA as a crosslinking agent (**Ref1**, **ER1-3**), clearly were able to store more energy elastically than epoxy resins with longer hardener, as depicted in **Figure 4a**. The same trend was observed by increasing the quantity of Jeff D230 in the formulation (**Figure 4b**), with a remarkable drop in E' in the range of 10-15 MPa, by comparing samples with E:H ratio 4:2 (**Ref2**, **ER4-6**) with samples E:H ratio 2:2 (**Ref5**, **ER13-15**). This fact can be related with the addition of a major number of long hardener linear chains and decreasing the hardener reactivity per amine group, which give more mobility to the system at high temperatures. It is precisely this enhanced polymer mobility in the rubbery state that allowed to evaluate deeply the contribution of lignin in the material network. As shown in **Figure 4a**, the incorporation of lignin to the flexible network that uses Jeff D400, resulted in the continuous increase of the crosslink density, raising the v_e value from 0.77 mmol/cm^3 for **Ref3** (0 % lignin) to 1.28 mmol/cm^3 for **ER9** (30 % lignin). The opposite case occurred for epoxy resins using the shortest hardener 1,6-HDA (**Ref1**); after small lignin inclusion (10 %, **ER1**), E' and consequently the crosslink density dropped drastically (around 30 MPa and 3 mmol/cm^3), which was attributed to a lignin disruption in the already compact original network for **Ref1**. Increasing the lignin content to 20 % seemed to improve slightly the crosslink density from 2.3 (**ER1**) to 2.7 mmol/cm^3 (**ER2**) without achieving **Ref1** v_e initial values (5.2 mmol/cm^3), and further lignin incorporation to 30 % for **ER3** collapsed again the system decreasing E' by 3.3 MPa. Epoxy resins

Ref2, **ER4**, **ER5**, and **ER6** using Jeff D230 as a hardener at an E:H ratio 4:2, exhibited a particular behavior; the system improved with 10 % lignin (**ER4**), while by increasing the lignin amount (20-30 %) was slightly detrimental for the crosslink system (**ER5-6**). Furthermore, as shown in **Figure 4b**, the addition of up to 30 % lignin increases the crosslink density for the formulations based on Jeff D230 with E:H ratios of 3:2 and 2:2. This is emphasized when comparing **Ref5**, with the lowest crosslink density (v_e = 0.2 mmol/cm^3) to **ER15** with a 40 % higher crosslink density (v_e = 0.7 mmol/cm^3) and 30 % lignin. These observations can help us adjust the formulation of the lignin-based epoxy resins to improve the material internal structure and, at the same time, enhance the biobased content.

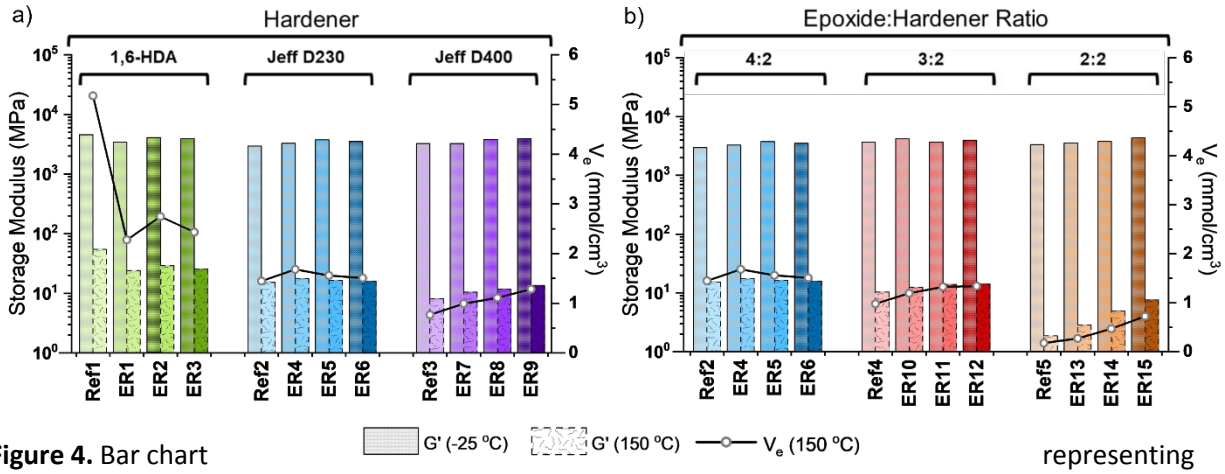

Figure 4. Bar chart representing storage modulus (E') at glassy region (-25 °C), storage modulus (E') at rubbery plateau and crosslink density (150 °C) versus epoxy resin samples with (a) different hardener and (b) different E:H ratio.

To further evaluate the mechanical properties of the lignin-based epoxy resins at large strains, tensile tests were carried out. Stress-strain curves are presented in **Figure 5** and **Figure S20-S24** (*Supporting Information),* and the data is summarized in **Table 1**. The stress-strain curves are very distinctive for each group of epoxy resins. As expected, they behave differently at room temperature upon mechanical strength depending on the hardener structure, E:H ratio, and lignin content in the formulation mixtures. Epoxy resins using 1,6-HDA as a crosslink agent (**Ref1**, **ER1-3**) exhibited a pronounced elastic response before break characteristic of brittle materials (**Figure 5a**), while samples containing Jeff D400 moieties (**Ref3**, **ER7-9**) displayed an initial elastic region, followed by an elastic limit point of maximum stress (yield point) that ultimately leads to

a plastic deformation before break, typical for ductile materials (**Figure 5b**). Similar trends were observed by decreasing the E:H ratio in epoxy resins based on Jeff D230 and by reducing the lignin content in the formulations; therefore, for clarity in the material comparison, the data extracted from the stress-strain curves was depicted in **Figure 6**. High Young Modulus values in the 1.0-2.5 GPa range were obtained, which are common results for epoxy resins containing linear hardeners. Interestingly, by exchanging the crosslinking agent in lignin-based samples from 1,6-HDA (**ER1-3**) to Jeff D230 (**ER4-6**), the elastic modulus remained constant or slightly increasing instead of decreasing, as can be observed in **Figure 6a**, passing from **Ref1** (2.2 GPa) to **Ref2** (1.9 GPa). This can be related with the contribution of lignin to the crosslink density, and for rigid reference networks (**Ref1**) this seemed to be detrimental. In contrast, lignin addition improved more flexible networks (**Ref2-3)**, as have been mentioned in the DMA discussion. Identical observation appeared in **Figure 6b**, with a small particularity, epoxy resins using 1,6-HDA as hardener (**Ref1, ER1-3**) not only exhibited the highest σ_{UTS} values (70-86 MPa) but also were the only samples that maximum stress and fracture of the sample coincided. Increasing the length of the hardener to Jeff D400 (**Ref3**, **ER7-9**) promoted the network flexibility, decreasing the elastic modulus between 0.1-0.2 GPa and the σ_{UTS} values from 6 to 12 MPa, in comparison with epoxy resins fabricated from Jeff D230 (**Ref2**, **ER4-6**). Remarkable was the ability of dissipating the stress applied via plastic deformation, as depicted in **Figure 6c**, especially in lignin-based epoxy resins fabricated with Jeff D400 (**ER7-9**), showing values of deformation before failure above 10 %, even with 30 % of lignin content.

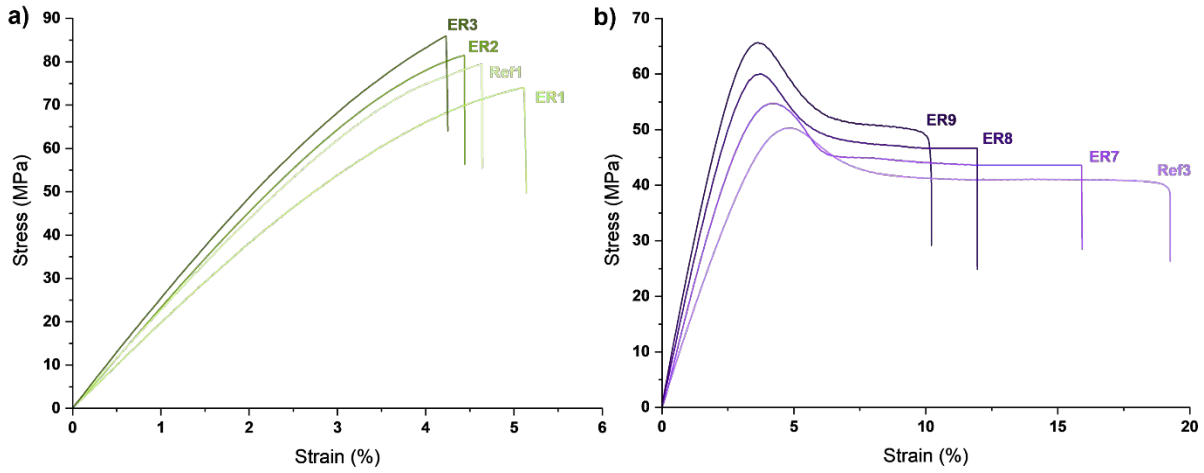

Figure 5. Stress-strain curves at 5 mm/min for a) **Ref1**, **ER1**, **ER2**, and **ER3**, and b) **Ref3**, **ER7**, **ER8**, and **ER9**.

In comparison with **Ref2**, **ER4**, **ER5**, and **ER6**, the reduction of r-DGEBA: Jeff D230 ratio (from 4:2 to 3:2 and 2:2, samples **Ref4-5**, **ER10-15**) led to materials with inferior elastic modulus, lower elastic limit, but enhanced the plastic response and the deformation to fracture, as observed in **Figure 6d-f**. These results agreed with previously mentioned statements that defended the increase in ductility of the materials by decreasing E:H ratio in their formulation, which provided lower crosslink density structure for the fabricated epoxy resins. The last parameter to evaluate was the effect of the lignin content on the tensile performance of the epoxy resin. Mostly all the systems behaved similarly, by increasing the lignin content from 0 to 30 %, the material became rigid, which increases the Young's modulus and the maximum stress, therefore reducing the plastic deformation before break. Noteworthy, the difference in the mechanical properties by exchanging the lignin amount in the formulation were greater for epoxy resins with more flexible network, such as **Ref3**, **ER7-9** and **Ref5**, **ER13-15**. Therefore, it confirmed the premise that lignin inclusion was beneficial or detrimental depending on the crosslink density of the reference r-DGEBA : hardener network, while elastic behavior was reduced from **Ref1** to **ER1**, was increased from **Ref2** to **ER4**, **Ref3** to **ER7**, **Ref4** to **ER11** and **Ref5** to **ER13** by only increasing 10 % lignin content in comparison with the reference system. This large comparison verified the mechanical behavior previously observed and gave an idea of the performance expected for each epoxy resin system in a real-life application.

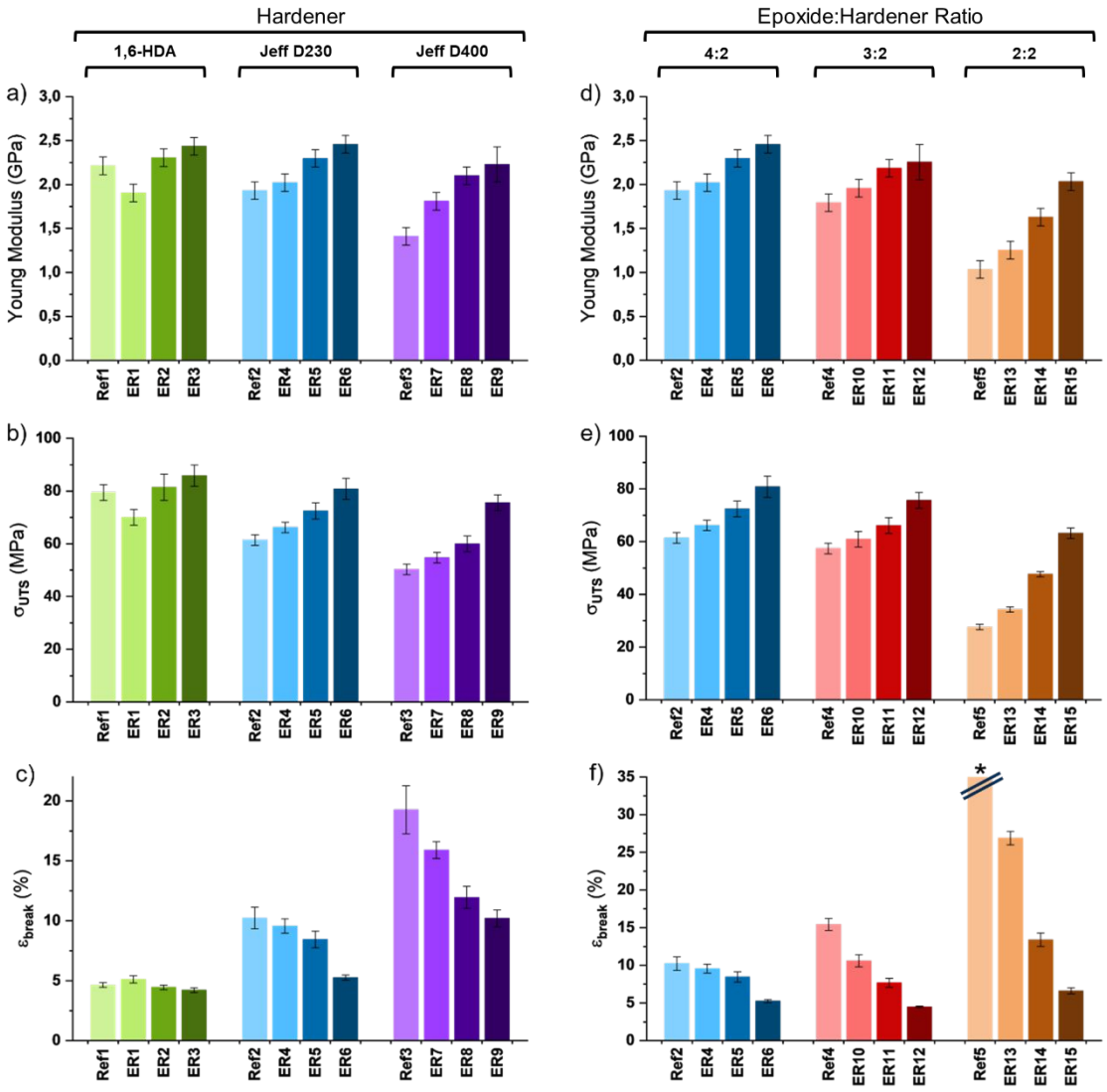

Figure 6. Bar chart representing Young's Modulus (a,d), the ultimate tensile strength (b,e) and fracture deformation (c,f) versus epoxy resin samples with (a,b,c) different hardener and (d,e,f) different E:H ratio. (*) ε_{break} = 89.2±5.0 % for **Ref5**.

Coating Fabrication and Cross Hatch Test

In order to evaluate the role the hardener plays for a specific application, the epoxy resin formulations presented in **Table 1** were coated on steel substrates at a constant flow rate. The coated plates were then thermally cured according to the conditions summarized in **Table S4**, producing a series of smooth, transparent, and amber-colored coatings as shown in **Tables S5-S9** (*Supporting Information*). The coatings had thicknesses ranging from 80-110 µm, displayed a

homogeneous and transparent appearance, glossy surface, and were without visible defects. The color of the coatings was directly related with the lignin content, generally varying from full transparent at 0 %, yellowish at 10 %, golden at 20 % and brown at 30 %. Besides, the E:H ratio influenced the volume of hardener used to disperse the lignin and for that reason coatings presented a lighter coloration by using 3:2 and 2:2 E:H ratio, respectively, instead of 4:2 ratio.

Additionally, the mechanical stability of the coatings on the substrate was analyzed by the surface crosshatch test. The methodology involves two different steps; first, the scratch step, where two perpendicular series of cuts were applied on the coating surface using a special utility knife with multiple parallel sharp blades, and second, the peeling step, which requires the adhesion of a tape on the crosshatch surface for specific period of time and further fast removal in a determined angle. The pictures of the coatings after scratch, after peeling, and the value ISO attributed after the crosshatch test are summarized in **Table S5-S9**.

The final results are compared in **Figure 7**. Considering that ISO value 0 (green), a perfect adhesion in steel substrate, and ISO value 5 (maroon), an incompatible union coating-substrate, remarkable trends related to the structure of the hardener, the lignin content, and the E:H ratio were extracted by comparing the different coating formulations. Better adhesion coating-substrate was achieved by increasing the length of the hardener, 1,6-HAD < Jeff D230 < Jeff D400, as shown in **Figure 7a**. This fact was attributed to the reduced crosslink density of the epoxy resin observed by DMA, yielding coatings with enhanced flexibility which allowed an improved resistance during the surface test. A similar tendency was observed by decreasing 4:2 to 2:2 the E:H ratio in the formulation, as a result, better adhesion was obtained for the coatings presenting more relaxed internal structure with an incremented quantity of hardener Jeff-D230 in the final material, as observed in **Figure 7b**. Interestingly, the influence between the formulation's lignin content and the resulting coatings' adhesion properties depended on how well the lignin interacted with the original r-DGEBA/hardener network. Consistent with what was previously mentioned in the thermal and mechanical properties section, the increased incorporation of lignin in r-DGEBA/Jeff D230 systems seems to have a dramatic effect on crosslink networks with shorter and fully reacted hardener (**ER4** > **ER5** > **ER6**). On the other hand, minor impacts on the adhesion coating-substrate quality were observed by including lignin to relaxed r-DGEBA/Jeff

D400 networks (**ER7**, **ER8** and **ER9**) and with formulations of r-DGEBA/Jeff D230 partially reacted (**ER13**, **ER14** and **ER15**). These results suggest that an accurate balance between hardener structure and ratio, as well as lignin content in the coating formulation could be determinant for a suitable coating-substrate adhesion.

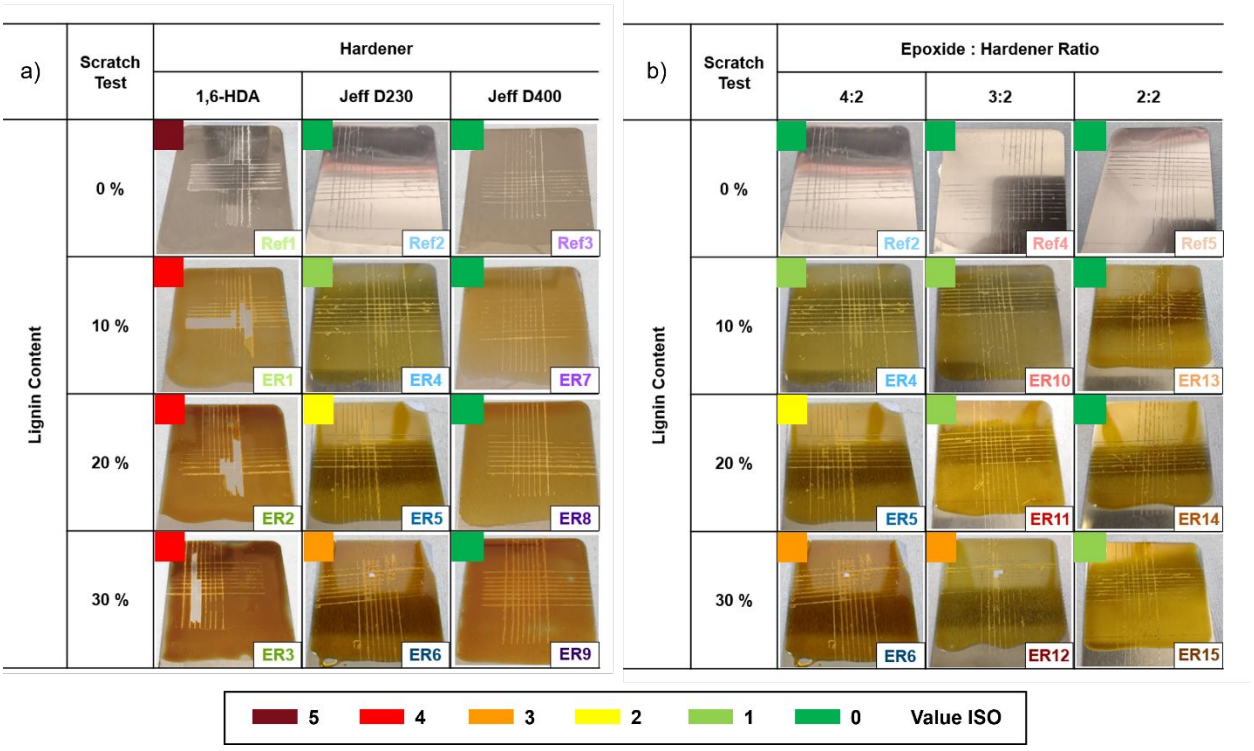

Figure 7. Surface scratch test of epoxy resin coatings with (**a**) different hardener and (**b**) different E:H ratio. Value ISO where 0 represent best adhesion and 5 represent worst adhesion coating/substrate.

CONCLUSIONS

In summary, **EKL** and **r-BPA** as waste-derived compounds have been used to produce **GEKL** and **r-BADGE**, respectively, using simple, efficient, and reproducible upcycling processes. We have characterized the epoxide monomer structures and tested thermally with different hardeners in order to evaluate the curing conditions and the uniformity of the final materials. Twenty epoxy resins were fabricated (**Ref1-5**, **ER1-15**) with different formulations by exchanging hardener structure (1,6-HDA, Jeff D230 and Jeff D400), E:H ratio (4:2, 3:2 and 2:2) and lignin content (0, 10, 20 and 30 %). Full curing was confirmed by the absence of exotherm in the DSC thermograms,

and the epoxy resins fabricated were characterized by FT-IR and DMA. The thermomechanical analysis revealed clear thermoset thermograms for all materials, with high storage modulus at glassy state (-25 ^{o}C, E'> 3GPa), followed by thermal transition and a final rubbery plateau. The crosslink density of the epoxy resins was determined at 150 ^{o}C, showing clear trends between formulations, such as a reduction of ν_e by increasing the length of the hardener structure or by decreasing the E:H ratio, for these cases, the samples exhibited lower T_g's and E' at rubbery state. Incrementing the lignin content altered differently the crosslink density of the materials, for networks using 1,6-HDA as a crosslinking agent, the lignin contribution was detrimental, while for systems containing a longer hardener or lower E:H ratio have experienced certain improvement by adding lignin. To further compare the mechanical behavior at standard conditions, tensile tests were performed. Except for the epoxy resins using 1,6-HDA as hardener that were clearly rigid with elastic responses that broke upon stress, all the other samples exhibited an elastic response, followed by a maximum in stress leading to a plastic dissipation before fracture. In general, using longer hardener or decreasing the E:H ratio in the formulation yielded epoxy resins with a smaller Young's modulus and lower σ_{UTS} while keeping plastic response to higher deformations before break. Finally, coatings on steel substrate were produced from the 20 different formulations, applying the previous knowledge of curing, and evaluating their appearance and adhesion properties.

The results extracted from the coating cross hatch tests confirmed that epoxy resins containing structures with lower crosslink density, due to the use of longer chain hardeners or a major amount of them, improved the adhesion of the coating. Additionally, these flexible systems can easily endure the addition of lignin (up to 20 %) and maintain their properties. This study provides an extensive comparison of how the final properties of lignin-based epoxy resins can be altered and predicted through exchanging formulation parameters related with the hardener, which ultimately will be the component that greatly affects the crosslink density of the covalent network and influences the performance of the material in specific applications.

ASSOCIATED CONTENT

Supporting Information: Information on general experimental details, synthetic procedures, epoxy resin fabrication, curing conditions, characterization, spectroscopic data, thermal, mechanical, and adhesion properties.

AUTHOR INFORMATION

Corresponding Author

*Email: marc.comibonachi@vito.be

*Email: richard.vendamme@vito.be

ACKNOWLEDGMENT

The authors gratefully acknowledge the research work done in LIGNICOAT and Cyclops projects. The LIGNICOAT project has received funding from the Bio-Based Industries Joint Undertaking under the European Union's Horizon 2020 research and innovation programme under the Grant Agreement No. 101023342. The JU receives support from the European Union's Horizon 2020 research and innovation programme and the Bio-based Industries Consortium. The Moonshot project CYCLOPS HBC.2021.0584 has received financial support of the Flemish Government and Flanders Innovation & Entrepreneurship (VLAIO).

REFERENCES

(1) Liu, J.; Wang, S.; Peng, Y.; Zhu, J.; Zhao, W.; Liu, X. Advances in sustainable thermosetting resins: From renewable feedstock to high performance and recyclability. *Progress in polymer science,* **2021**, *113*, 101353. DOI: 10.1016/j.progpolymsci.2020.101353

(2) Gonçalves, F. A.; Santos, M.; Cernadas, T.; Ferreira, P.; Alves, P. Advances in the development of biobased epoxy resins: insight into more sustainable materials and future applications. *International Materials Reviews,* **2022**, *67*, 2, 119-149. DOI: 10.1080/09506608.2021.1915936

(3) Lu, X.; Gu, X. A sustainable lignin-based epoxy resin: Its preparation and combustion behaviors. *Industrial Crops and Products,* **2023**, *192*, 116151. DOI: 10.1016/j.indcrop.2022.116151

(4) Jiang, T.-W.; Reddy, K. S. K.; Chen, Y.-C.; Wang, M.-W.; Chang, H.-C.; Abu-Omar, M. M.; Lin, C.-H. Recycling waste polycarbonate to bisphenol A-based oligoesters as epoxy-curing agents, and degrading epoxy thermosets and carbon fiber composites into useful chemicals. *ACS Sustainable Chemistry & Engineering* **2022**, *10*, 7, 2429-2440. DOI: 10.1016/j.jobab.2024.01.003

(5) Yu, E.; Jan, K.; Chen, W.-T. Separation and Solvent Based Material Recycling of Polycarbonate from Electronic Waste. *ACS Sustainable Chemistry & Engineering* **2023**, *11*, 34, 12759-12770. DOI: 10.1021/acssuschemeng.3c03152

(6) Romani, A.; Levi, M.; Pearce, J. M. Recycled polycarbonate and polycarbonate/acrylonitrile butadiene styrene feedstocks for circular economy product applications with fused granular fabrication-

based additive manufacturing. *Sustainable Materials and Technologies,* **2023**, *38*, e00730. DOI: 10.2139/ssrn.4508039

(7) Parida, D.; Aerts, A.; Vanbroekhoven, K.; Van Dael, M.; Mitta, H.; Li, L.; Eevers, W.; Van Geem, K. M.; Feghali, E.; Elst, K. Monomer recycling of polyethylene terephthalate, polycarbonate and polyethers: scalable processes to achieve high carbon circularity. *Progress in Polymer Science,* **2023**, 101783. DOI: 10.1016/j.progpolymsci.2023.101783.

(8) Hu, L.-C.; Oku, A.; Yamada, E. Alkali-catalyzed methanolysis of polycarbonate. A study on recycling of bisphenol A and dimethyl carbonate. *Polymer,* **1998**, *39* (16), 3841-3845. DOI: 10.1016/S0032-3861(97)10298-1

(9) Liu, F.-S.; Li, Z.; Yu, S.-T.; Cui, X.; Xie, C.-X.; Ge, X.-P. Methanolysis and hydrolysis of polycarbonate under moderate conditions. *Journal of Polymers and the Environment,* **2009**, *17*, 208-211. DOI: 10.1007/s10924-009-0140-0

(10) Kim, J. G. Chemical recycling of poly (bisphenol A carbonate). *Polymer Chemistry,* **2020**, *11* (30), 4830-4849. DOI: 10.1039/C9PY01927H

(11) Zhou, X.; Zhai, Y.; Ren, K.; Cheng, Z.; Shen, X.; Zhang, T.; Bai, Y.; Jia, Y.; Hong, J. Life cycle assessment of polycarbonate production: Proposed optimization toward sustainability. *Resources, Conservation and Recycling,* **2023**, *189*, 106765. DOI: 10.1016/j.resconrec.2022.106765

(12) Verdugo, P.; Santiago, D.; De la Flor, S.; Serra, À. A Biobased Epoxy Vitrimer with Dual Relaxation Mechanism: A Promising Material for Renewable, Reusable, and Recyclable Adhesives and Composites. *ACS Sustainable Chemistry & Engineering* **2024**, *12*, 15, 5965-5978. DOI: 10.1021/acssuschemeng.4c00205.

(13) Kalita, D. J.; Tarnavchyk, I.; Kalita, H.; Chisholm, B. J.; Webster, D. C. Novel bio-based epoxy resins from eugenol derived copolymers as an alternative to DGEBA resin. *Progress in Organic Coatings* **2023**, *178*, 107471. DOI: 10.1016/j.porgcoat.2023.107471.

(14) Chen, C.-H.; Tung, S.-H.; Jeng, R.-J.; Abu-Omar, M. M.; Lin, C.-H. A facile strategy to achieve fully bio-based epoxy thermosets from eugenol. *Green chemistry* **2019**, *21*, 16, 4475-4488. DOI: 10.1039/C9GC01184F

(15) Fang, Z.; Nikafshar, S.; Hegg, E. L.; Nejad, M. Biobased divanillin as a precursor for formulating biobased epoxy resin. *ACS sustainable chemistry & engineering* **2020**, *8*, 24, 9095-9103. DOI: 10.1021/acssuschemeng.8b02419

(16) Martinez-Hernandez, E.; Cui, X.; Scown, C. D.; Amezcua-Allieri, M. A.; Aburto, J.; Simmons, B. A. Techno-economic and greenhouse gas analyses of lignin valorization to eugenol and phenolic products in integrated ethanol biorefineries. *Biofuels, Bioproducts and Biorefining* **2019**, *13*, 4, 978-993. DOI: 10.1002/bbb.1989

(17) Pappa, C.; Feghali, E.; Vanbroekhoven, K.; Triantafyllidis, K. S. Recent advances in epoxy resins and composites derived from lignin and related bio-oils. *Current Opinion in Green and Sustainable Chemistry,* **2022**, 100687. DOI: 10.1016/j.cogsc.2022.100687

(18) Lu, X.; Gu, X. A review on lignin-based epoxy resins: Lignin effects on their synthesis and properties. *International Journal of Biological Macromolecules,* **2023**, 229, 778-790. DOI: 10.1016/j.ijbiomac.2022.12.322

(19) Dessbesell, L.; Paleologou, M.; Leitch, M.; Pulkki, R.; Xu, C. C. Global lignin supply overview and kraft lignin potential as an alternative for petroleum-based polymers. *Renewable and Sustainable Energy Reviews,* **2020**, *123*, 109768. DOI: 10.1016/j.rser.2020.109768

(20) Sethupathy, S.; Morales, G. M.; Gao, L.; Wang, H.; Yang, B.; Jiang, J.; Sun, J.; Zhu, D. Lignin valorization: Status, challenges and opportunities. *Bioresource Technology* **2022**, *347*, 126696. DOI: 10.1016/j.biortech.2022.126696

(21) Lawoko, M.; Samec, J. S. Kraft lignin valorization: Biofuels and thermoset materials in focus. *Current Opinion in Green and Sustainable Chemistry,* **2022**, 100738. DOI: 10.1016/j.cogsc.2022.10073

(22) Zou, S.-L.; Xiao, L.-P.; Li, X.-Y.; Yin, W.-Z.; Sun, R.-C. Lignin-based composites with enhanced mechanical properties by acetone fractionation and epoxidation modification. *Iscience,* **2023**, *26*, 3. DOI: 10.1016/j.isci.2023.106187

(23) Gioia, C.; Lo Re, G.; Lawoko, M.; Berglund, L. Tunable thermosetting epoxies based on fractionated and well-characterized lignins. *Journal of the American Chemical Society,* **2018**, *140*, 11, 4054-4061. DOI: 10.1021/jacs.7b13620

(24) Silau, H.; Melas, A.; Dam-Johansen, K.; Wu, H.; Daugaard, A. E.; Høj, M. Solvent Fractionation and Depolymerization Provide Liquid Lignin Fractions Exploited as Bio-based Aromatic Building Blocks in Epoxies. *ACS Sustainable Chemistry & Engineering,* **2023**, *11*, 4, 1591-1597. DOI: 10.1021/acssuschemeng.2c06668

(25) Gioia, C.; Colonna, M.; Tagami, A.; Medina, L.; Sevastyanova, O.; Berglund, L. A.; Lawoko, M. Lignin-Based Epoxy Resins: Unravelling the Relationship between Structure and Material Properties. *Biomacromolecules,* **2020**, *21*, 5, 1920-1928. DOI: 10.1021/acs.biomac.0c00057.

(26) Tang, R.; Xue, B.; Tan, J.; Guan, Y.; Wen, J.; Li, X.; Zhao, W. Regulating lignin-based epoxy vitrimer performance by fine-tuning the lignin structure. *ACS Applied Polymer Materials,* **2022**, *4*, 2, 1117-1125. DOI: 10.1021/acsapm.1c01541

(27) Li, X.-Y.; Xiao, L.-P.; Zou, S.-L.; Xu, Q.; Wang, Q.; Lv, Y.-H.; Sun, R.-C. Preparation and Characterization of Bisphenol A-Based Thermosetting Epoxies Based on Modified Lignin. *ACS Applied Polymer Materials,* **2023**, *5*, 5, 3611-3621. DOI: 10.1021/acsapm.3c00262

(28) Xue, B.; Tang, R.; Xue, D.; Guan, Y.; Sun, Y.; Zhao, W.; Tan, J.; Li, X. Sustainable alternative for bisphenol A epoxy resin high-performance and recyclable lignin-based epoxy vitrimers. *Industrial Crops and Products,* **2021**, *168*, 113583. DOI: 10.1016/j.indcrop.2021.113583.

(29) Sreejaya, M.; Sankar, R. J.; Ramanunni, K.; Pillai, N. P.; Ramkumar, K.; Anuvinda, P.; Meenakshi, V.; Sadanandan, S. Lignin-based organic coatings and their applications: A review. *Materials Today: Proceedings,* **2022**, *60*, 494-501. DOI: 10.1021/acssuschemeng.3c00889

(30) Boarino, A.; Charmillot, J.; Figueirêdo, M. B.; Le, T. T. H.; Carrara, N.; Klok, H.-A. Ductile, High-Lignin-Content Thermoset Films and Coatings. *ACS Sustainable Chemistry & Engineering,* **2023**. DOI: 10.1021/acssuschemeng.3c03030.

(31) Thys, M.; Kaya, G. E.; Soetemans, L.; Van Assche, G.; Bourbigot, S.; Baytekin, B.; Vendamme, R.; Van den Brande, N. Bioaromatic-Associated Multifunctionality in Lignin-Containing Reversible Elastomers. *ACS Applied Polymer Materials,* **2023**, *5* (8), 5846-5856. DOI: 10.1021/acsapm.3c00491.

(32) Zhou, Y.; Jiang, C.; Zhang, Y.; Liang, Z.; Liu, W.; Wang, L.; Luo, C.; Zhong, T.; Sun, Y.; Zhao, L.; et al. Structural Optimization and Biological Evaluation of Substituted Bisphenol A Derivatives as β-Amyloid Peptide Aggregation Inhibitors. *Journal of Medicinal Chemistry,* **2010**, *53* (15), 5449-5466. DOI: 10.1021/jm1000584.

(33) Meng, X.; Crestini, C.; Ben, H.; Hao, N.; Pu, Y.; Ragauskas, A. J.; Argyropoulos, D. S. Determination of hydroxyl groups in biorefinery resources via quantitative 31P NMR spectroscopy. *Nature Protocols,* **2019**, *14* (9), 2627-2647. DOI: 10.1038/s41596-019-0191-1.

(34) Gracia-Vitoria, J.; Rubens, M.; Feghali, E.; Adriaensens, P.; Vanbroekhoven, K.; Vendamme, R. Low-field benchtop versus high-field NMR for routine 31P analysis of lignin, a comparative study. *Industrial Crops and Products,* **2022**, *176*, 114405. DOI: 10.1016/j.indcrop.2021.114405

(35) Zhao, S.; Abu-Omar, M. M. Renewable Thermoplastics Based on Lignin-Derived Polyphenols. *Macromolecules,* **2017**, *50* (9), 3573-3581. DOI: 10.1021/acs.macromol.7b00064.

(36) Over, L. C.; Grau, E.; Grelier, S.; Meier, M. A. R.; Cramail, H. Synthesis and Characterization of Epoxy Thermosetting Polymers from Glycidylated Organosolv Lignin and Bisphenol A. *Macromolecular Chemistry and Physics,* **2017**, *218* (4), 1600411. DOI: 10.1002/macp.201600411.

(37) Xin, J.; Li, M.; Li, R.; Wolcott, M. P.; Zhang, J. Green Epoxy Resin System Based on Lignin and Tung Oil and Its Application in Epoxy Asphalt. *ACS Sustainable Chemistry & Engineering,* **2016**, *4* (5), 2754-2761. DOI: 10.1021/acssuschemeng.6b00256.

(38) Sabu, M.; Bementa, E.; Jaya Vinse Ruban, Y.; Ginil Mon, S. A novel analysis of the dielectric properties of hybrid epoxy composites. *Advanced Composites and Hybrid Materials,* **2020**, *3*, 325-335. DOI: 10.1007/s42114-020-00166-0

(39) Prado, R.; Erdocia, X.; De Gregorio, G. F.; Labidi, J.; Welton, T. Willow lignin oxidation and depolymerization under low cost ionic liquid. *ACS Sustainable Chemistry & Engineering,* **2016**, *4,* 10, 5277-5288. DOI: 10.1021/acssuschemeng.6b00642

(40) García, A.; Erdocia, X.; Alriols, M. G.; Labidi, J. Effect of ultrasound treatment on the physicochemical properties of alkaline lignin. *Chemical Engineering and Processing: Process Intensification,* **2012**, *62*, 150-158. DOI: 10.1016/j.cep.2012.07.011

(41) Gordobil, O.; Delucis, R.; Egüés, I.; Labidi, J. Kraft lignin as filler in PLA to improve ductility and thermal properties. *Industrial Crops and Products,* **2015**, *72*, 46-53. DOI: 10.1016/j.indcrop.2015.01.0553.

Graphical Abstract (TOC)

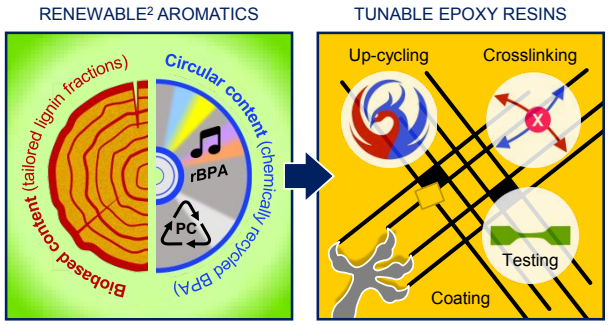

Synopsis:

This study investigates the combined sustainable use of recycled and biobased building blocks to deliver renewable materials with improved properties.